

Characterisation of edge filamentary structures in the 3D geometry of Wendelstein 7-X limiter plasmas

G. Kocsis¹, A. Alonso², C. Biedermann³, G. Cseh¹, A. Dinklage³, O. Grulke³, M. Jakubowski³,
R. König³, M. Krychowiak³, M. Otte³, T. Sunn Pedersen³, T. Szepesi¹, U. Wenzel³,
P. Xanthopoulos³, S. Zoletnik¹ and the W7-X Team

¹*Wigner RCP RMI, Budapest, Hungary*

²*CIEMAT, Madrid, Spain*

³*Max-Planck-Institute for Plasma Physics, Greifswald, Germany*

Turbulent structures elongated along the magnetic field lines are observed in many different magnetized plasmas, including fusion plasmas of tokamaks and stellarators. Those structures, often referred to as blobs/filaments, are investigated typically in the scrape-off layer (SOL) and at the plasma edge inside the last closed flux surface (LCFS).

The magnetic field of the Wendelstein 7-X (W7-X) stellarator was optimised to minimise the neoclassical loss channels. Due to the 3D geometry of the resulting magnetic field, the turbulence drives, thus the anomalous transport, might be different from axisymmetric tokamaks. For example gyrokinetic simulations have revealed that ITG turbulence is also expected to display peculiar properties in this device: the fluctuations appear localized both in the poloidal and the parallel direction, as they cannot go past a single module of the stellarator [1]. These properties and a sophisticated video diagnostic system combined with gas puff imaging offered a good opportunity to search for anomalous turbulent phenomena even in the first initial experimental phase of W7-X operation (OP1.1), and this study is summarised in this contribution.

In OP1.1 experiments were performed in limiter configuration with Helium and Hydrogen fuelled plasmas heated by ECRH up to 4.3 MW [2]. The installation of plasma facing components was kept to a minimum with only five symmetrically mounted inboard graphite limiters. As a consequence of the almost 'naked' vacuum vessel, an outgassing reservoir of primarily Hydrogen is generated during the experimental day, and depending on the conditions (wall temperature) neutral gas is released causing a slow density increase which - at later phase of the discharges - could act as 'global' gas puff for the video observation, making e.g. filamentary structures visible. Often the discharges are terminated by the particle influx generated radiation collapse.

A ten channel overview video diagnostic system [3] observing the visible radiation of the plasma is also installed in ten tangential views around the torus. During OP1.1 plasma experiments two different types of cameras were used in the system: the workhorses were the EDICAM cameras (~400frames/s @1.3Mpixel) recording the plasma shape and size at low speed while also monitoring in parallel smaller Regions of Interest (ROI) at up to 5 kHz. One tangential port was equipped with a fibre bundle (500x700fibres) attached to a fast framing

camera (Photron SA5, 7kframe/s @ 1Mpixel) which was used in the studies presented here at 46.5kHz frame rate allowing us to observe the plasma for a toroidal range of about 50°.

Observation with the tangentially viewing video cameras showed that the visible radiation of these limiter plasmas is concentrated in a narrow layer/belt around a specific magnetic flux surface [4]. The typical perpendicular/radial extension of this radiation belt is about 10% of the effective radius of the LCFS. Assuming homogeneous radiation distribution on flux surface, the effective radius of the central magnetic surface of the radiating belt could be determined from the tangential camera images by taking into account the projection properties of the camera view and the geometry of the vacuum magnetic flux surfaces [4]. The radial position of the belt is changing during the discharge: at the breakdown it is located at the inner half of plasma radius, then it expands within 50ms through the LCFS into the scrape of layer (SOL), where the typical electron temperature is a few tens of eV. When the influx of neutrals increases the plasma edge cools and this radiating belt moves back inside the LCFS, and finally during the radiation collapse it shrinks to the plasma centre.

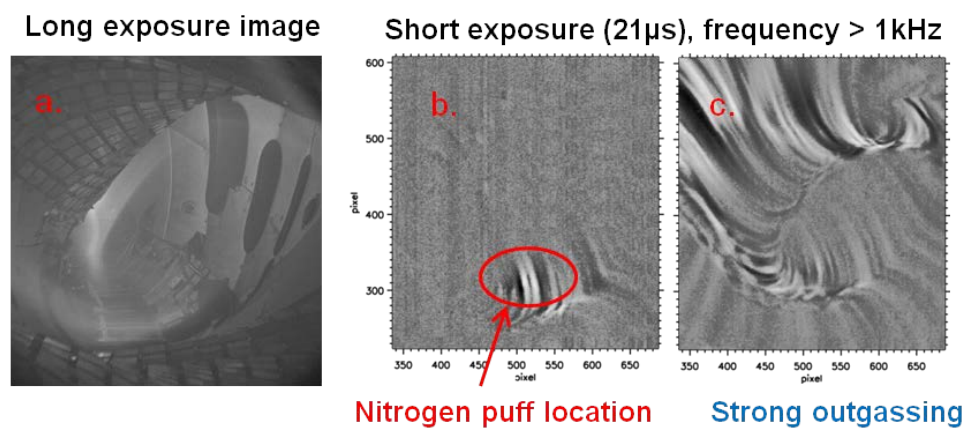


Fig.1. Long exposure (10ms) image (a.) and two short exposure (21µs, frequency > 1kHz) images during Nitrogen gas puff (b.) and at the strong wall outgassing case (c.).

When the plasma light emission was intense enough and therefore the exposure time could be reduced below 200 µs, the apparent homogeneous radiation of the magnetic surface breaks down into large structures elongated along the magnetic field lines (filaments, see fig.1.). Such a highly radiating and poloidally rotating filamentary layer was typically observed during breakdown and at later phase of the discharges in the ‘global gas puffing’ case (fig.1c.) caused by wall recycling. In these cases the radiating layer was always located in the confined plasma. If the radial position of the radiating belt - measured by the video cameras - was outside the LCFS the filaments could be visualised only by additional local puffing of Nitrogen (see fig.1b). Such a gas puff system was installed at the bottom of W7-X and was in the view of the fast tangential observation [5]. The enhanced radiation provoked by the cloud of the puffed Nitrogen was localised both poloidally and toroidally. EMC3-EIRENE simulation of these Nitrogen gas puff experiments confirmed the video observation, that most of the H α and the impurity radiation is located in the SOL [6].

Independently of the radial position of the radiating belt (both inside and outside of the LCFS) the evolution of the radiation shows a fluctuating behaviour in areas where filaments are seen. This light fluctuation is the consequence of the local electron density fluctuation caused by high density filaments crossing the observation volume. Typically, the RMS fluctuation amplitude is around 10% and the skewness of the probability density function is positive, that is the filaments show blobby behaviour. The power spectrum is a broadband spectrum which is concentrated in a frequency range of 1-10kHz, indicating that the observed phenomenon is a series of individual events (filaments) which are born and seen by the camera at random times. The decorrelation time is shorter than 100 μ s.

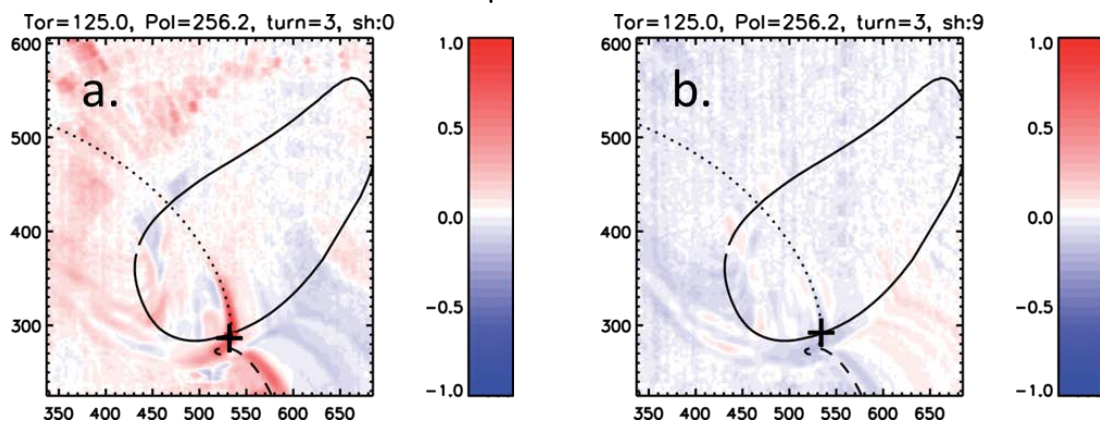


Fig.2. Cross correlation of the movie with the signal of the reference point (+) obtained from the projection of a predefined point of the radiating magnetic surface at zero time lag (a.) and at 180 μ s (b.) where the correlation already vanished. The radiating surface is in the SOL (reff=0.505m). Field line tracing starting from the reference point is also over plotted (dotted: forward, dashed: backward) for three toroidal turns in both directions, but the field lines hit the limiters within one turn. The black contour represents the projection of a poloidal cut of the magnetic surface at 125° toroidal angle.

The 2D imaging allows us to calculate 2D cross correlation ‘images’ for different time lags (fig.2 and 3.). A reference point was selected at a given toroidal and poloidal angle on the radiating magnetic surface, which was projected onto the camera image (marked by + on fig.2. and fig.3.). The light signal of this reference point was used for the cross correlation calculation. If the radiating belt is in the SOL and gas puff is applied the zero time lag correlation image shows a highly correlating structure which follows the magnetic field line traced from the reference points (fig.2a). By shifting the time lag this high correlation zone moves poloidally relative to the reference field line (see e.g fig.3), showing that the filament moves poloidally. The poloidal velocity is consistent with an ExB advection of the filaments with a $E_R \sim 2-5$ kV/m. The radial electric field is found positive if the magnetic surface (and the filament) is in the SOL and negative if the surface is in the confined plasma. The sign of the radial electric field is in line with neoclassical calculations and also confirmed by reflectometry measurements [7].

In the SOL filaments could only be visualised by gas puff therefore their ‘visibility’ is limited both poloidally and toroidally to the extension of the gas cloud. In this case we could not estimate the B-parallel length of the filaments but they are probably longer than the toroidal range of their visibility. In contrary, in the ‘global gas puffing’ case when the radiating layer and the filaments are inside the LCFS, they are seen at any poloidal angle on the camera images, and the 2D cross correlation ‘image’ shows that they are extended over two toroidal turns both in the forward and backward toroidal directions (fig.3.).

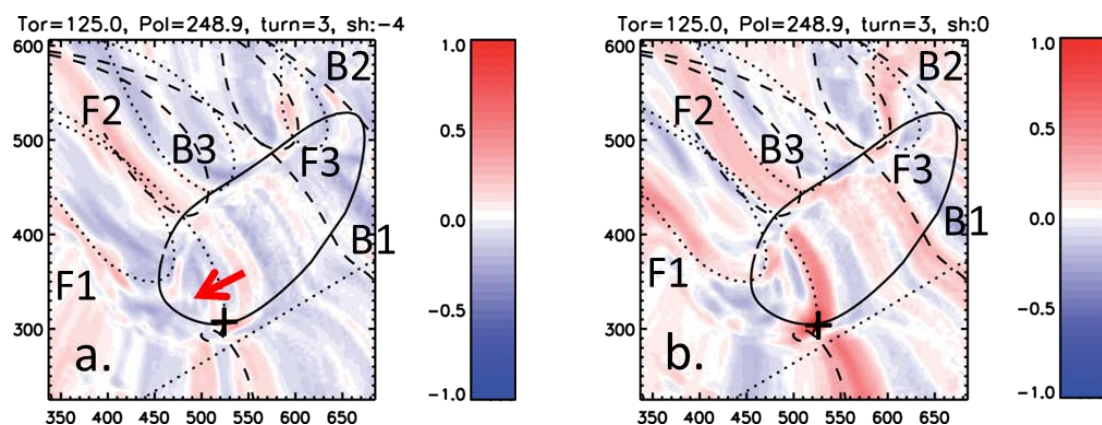


Fig.3. Cross correlation of the movie with the signal of the reference pixel (+) at $-80\mu\text{s}$ (a.) and at zero (b.) time lag. The radiating surface is in the confined plasma (normalised effective radius ~ 0.85). Field line tracing starting from the reference point is also over plotted (dotted: forward, dashed: backward) for three toroidal turns in both directions. The black contour represents the poloidal cut of the surface at 125° toroidal angle.

Our observation of filamentary structures in the plasma edge do not show an obvious poloidal and toroidal localisation of light fluctuation levels, which excludes the possibility of a relation between the observed filamentary structure and ITG turbulence. Another probable candidate might be TEM turbulence - expected to dominate at outer radii in view of the strong density gradient - which shares similar scales with ITG, but is known to be significantly more dispersed, due to the multiple trapping regions overlapping with the bad curvature in the stellarator [8]. However the long B-parallel extension of the filaments may suggest that the instability is more interchange-like than drift-wave turbulence. Additionally the conditions (e.g. T_e) are probably similar in the edge and SOL regions where the filaments are visible except the B parallel extension of the plasma covering by the filament. This parallel extension can be also longer than one toroidal turn in the SOL, too. Accordingly, the filament crosses both good and bad curvature regions ($\iota \sim 0.8-0.9$) which may explain the lack of the poloidal localisation for the bad curvature regions expected for interchange-like instability.

It is worth to mention that a proof of principle measurement was also performed with two EDICAMs monitoring smaller Regions of Interest (ROI) at 5 kHz. These cameras also revealed correlation between the light signals detected in neighbouring modules.

Based on our investigations in OP1.1 this study will be continued in the next W7-X experimental campaign with an extended diagnostic set-up. Almost all views of the overview video diagnostics will be prepared to measure the light fluctuation with 10-50kHz frame rate which may reveal more details in 3D about these turbulent structures, if the plasma radiation intensity allows fast enough framing.

“This work has been carried out within the framework of the EUROfusion Consortium and has received funding from the Euratom research and training programme 2014-2018 under grant agreement No 633053. The views and opinions expressed herein do not necessarily reflect those of the European Commission.”

- [1] P. Xanthopoulos et al. PRX 6 (2016) 021033
- [3] G. Kocsis et al. FED 96-97 (2015) 808
- [5] T. Barbui et al. RSI 87 (2016) 11E554
- [7] A. Krämer-Flecken et al. NF 57 (2017) 066023

- [2] R.C. Wolf et al. submitted to NF
- [4] T. Szepesi et al. P5.119, this conference
- [6] F. Effenberg et al. NF 57 (2017) 036021
- [8] J.H.E. Proll et al. PP 20 (2013) 122506